

Supplementary Information

Self-assembly of amorphous calcium carbonate microlens arrays

Kyubock Lee^{1,3}, Wolfgang Wagermaier¹, Admir Masic¹, Krishna P. Kommareddy¹,
Mathieu Bennet¹, Inderchand Manjubala^{1,5}, Seung-Woo Lee², Seung B. Park³, Helmut
Cölfen⁴, Peter Fratzl^{1,*}

¹Department of Biomaterials, Max Planck Institute of Colloids and Interfaces, 14424
Potsdam, Germany

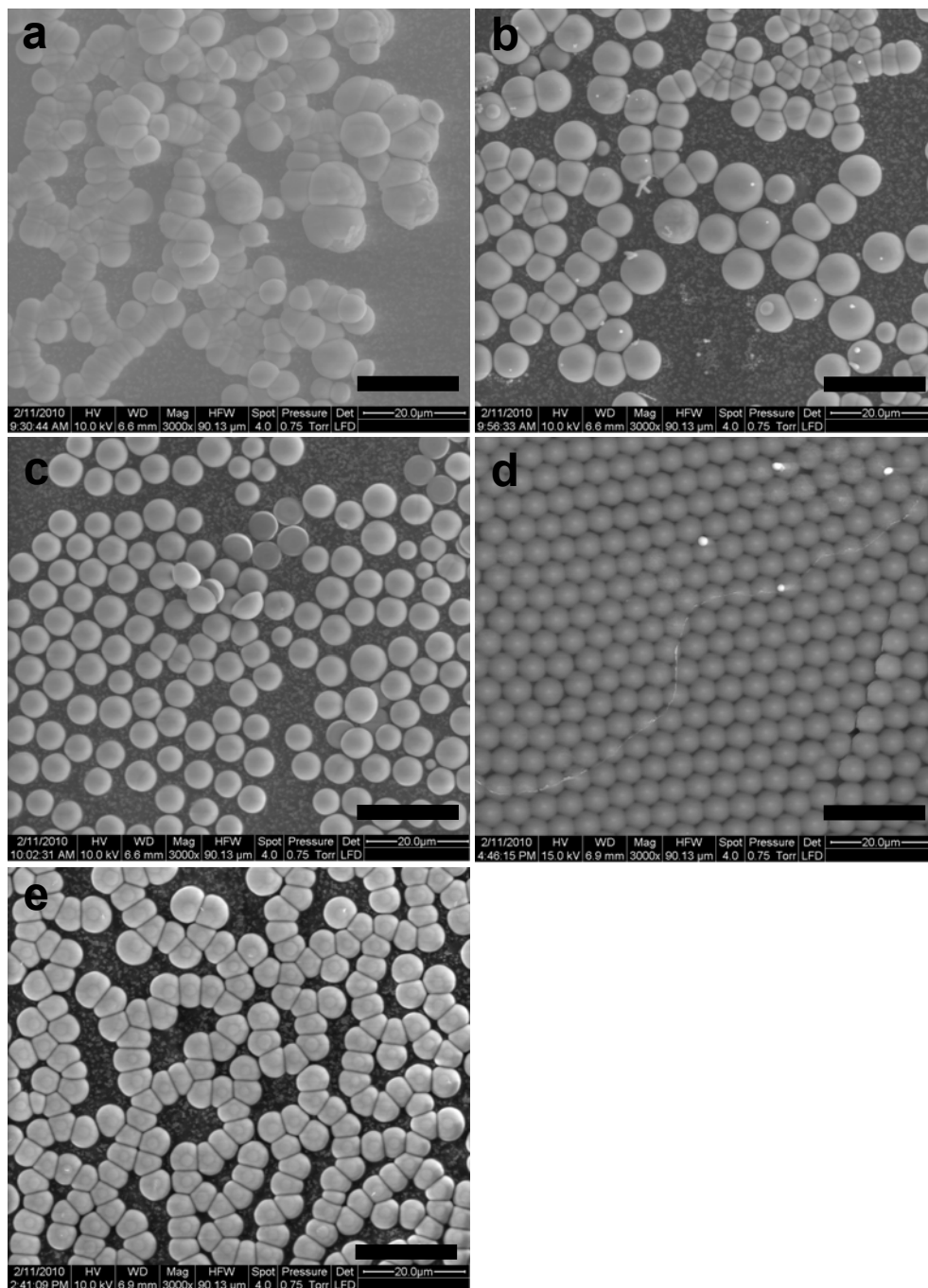
²CO₂ Sequestration Research Department, Korea Institute of Geoscience and Mineral
Resources, Daejeon 305-350, South Korea

³Department of Chemical and Biomolecular Engineering, KAIST, Daejeon 305-701,
South Korea

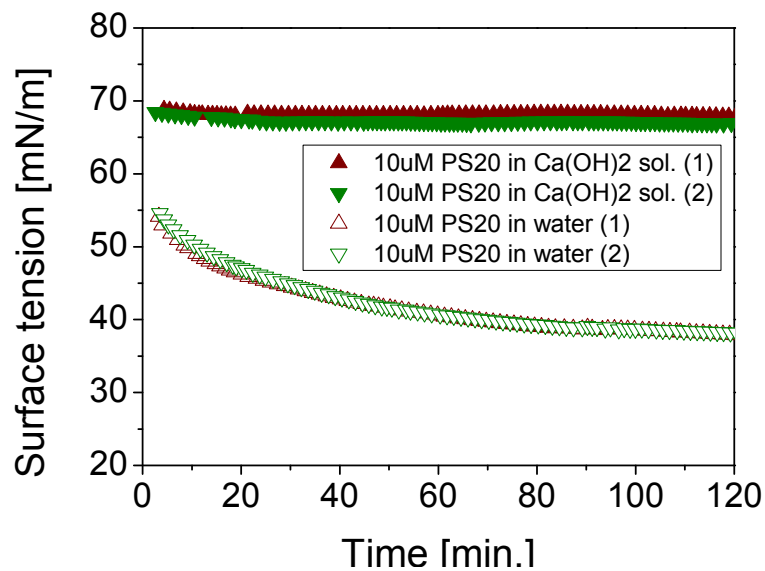
⁴Physical Chemistry, University of Konstanz, D-78457 Konstanz, Germany

⁵Biomedical Engineering Division, Centre for Biomedical Research, School of Bio-
Sciences and Technology, VIT University, 632 014, Vellore, Tamilnadu, India

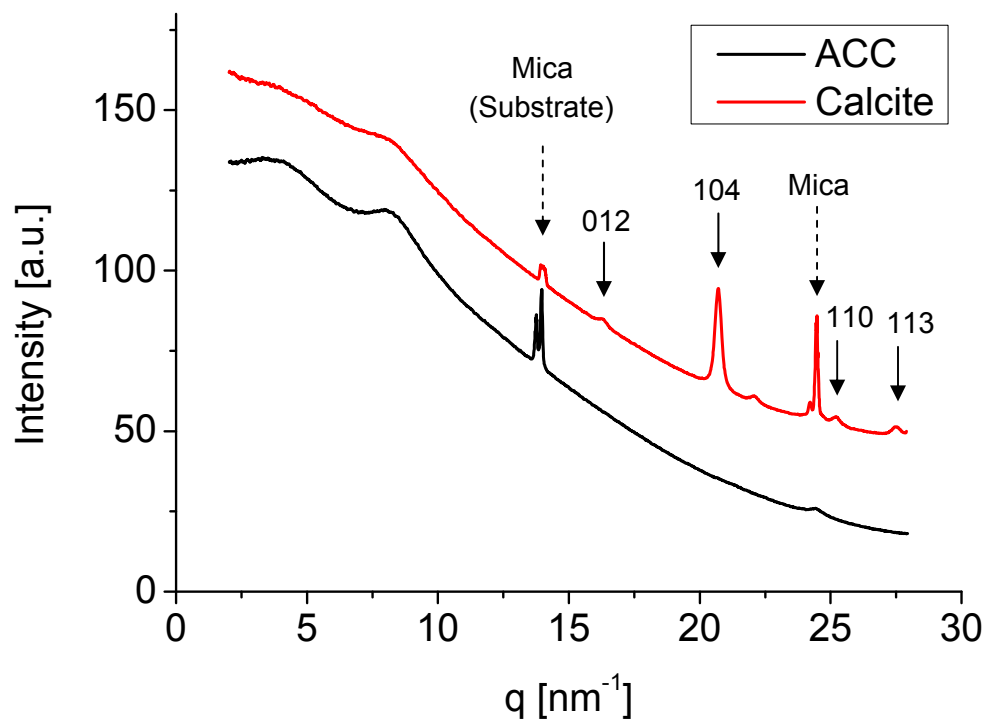
* Corresponding author: P. Fratzl (fratzl@mpikg.mpg.de)



Supplementary Figure S1. SEM images of CaCO_3 microlens structures formed at various concentrations of polysorbate 20. a-e, 0, 3, 6, 10 and 50 μM , respectively. The morphology of CaCO_3 microlenses becomes uniform in the presence of polysorbate 20 and shows a hexagonally packed array at 10 μM . At the higher concentration, CaCO_3 microlenses start to stick to each other in the early stage and grow up to form chain-like structures. All the scale bars are 20 μm .

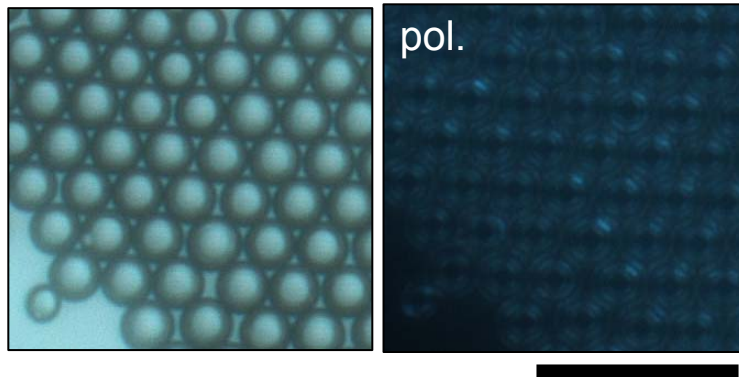


Supplementary Figure S2. Surface tension measurements. Surface tension of Ca(OH)₂ solution and water equally containing 10 μM of polysorbate 20. The surface tension of Ca(OH)₂ solution with 10 μM of polysorbate is close to that of pure water (71.97 mN/m at 25 °C), which means that most of the surfactant molecules are adsorbed on the CaCO₃ precipitates and agglomerates and very little amounts of them are left in the solution. The critical micelle concentration of polysorbate 20 is 80 μM.

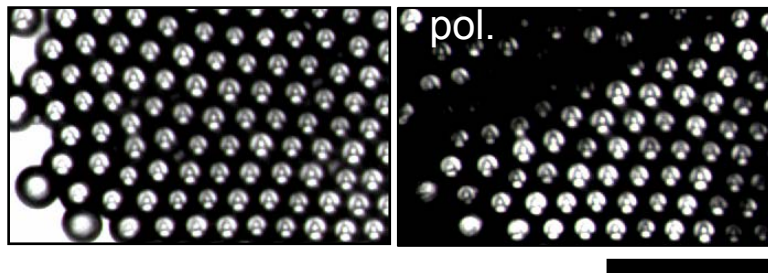


Supplementary Figure S3. X-ray diffraction patterns of the ACC and calcitic microlens array. ACC microlens array does not show any peaks except peaks from Mica substrate indicated by arrows with dashed-line. ACC Microlens array is crystallized into calcite by thermal heating over 300 °C.

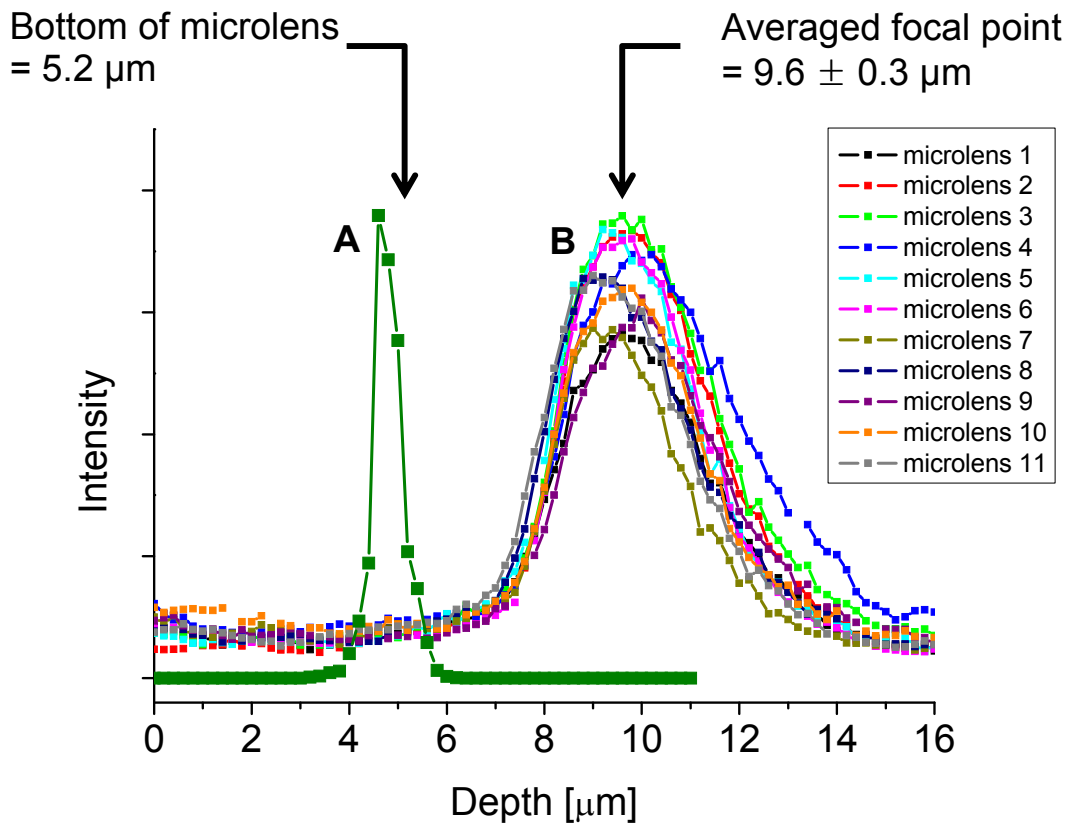
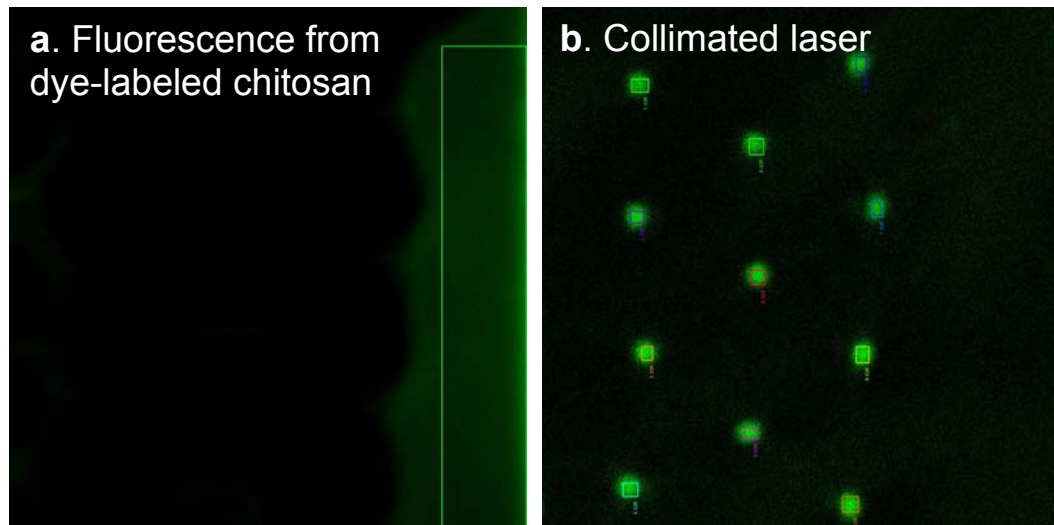
a. Amorphous CaCO_3 microlens array



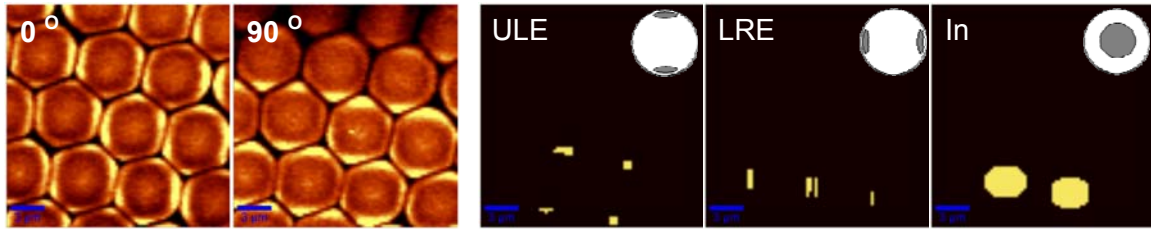
b. Calcitic microlens array



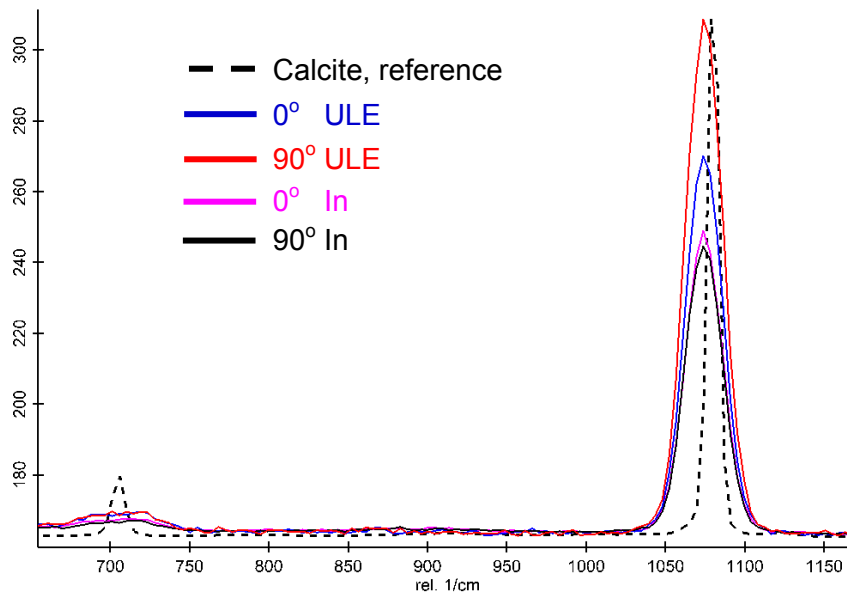
Supplementary Figure S4. Optical microscope images of ACC and calcitic microlens arrays. Images on right side show the same areas of left images under cross polarization of light. The projected image of the ‘A’ array in **b** is observed through calcitic microlens array. All the scale bars are 25 μm .



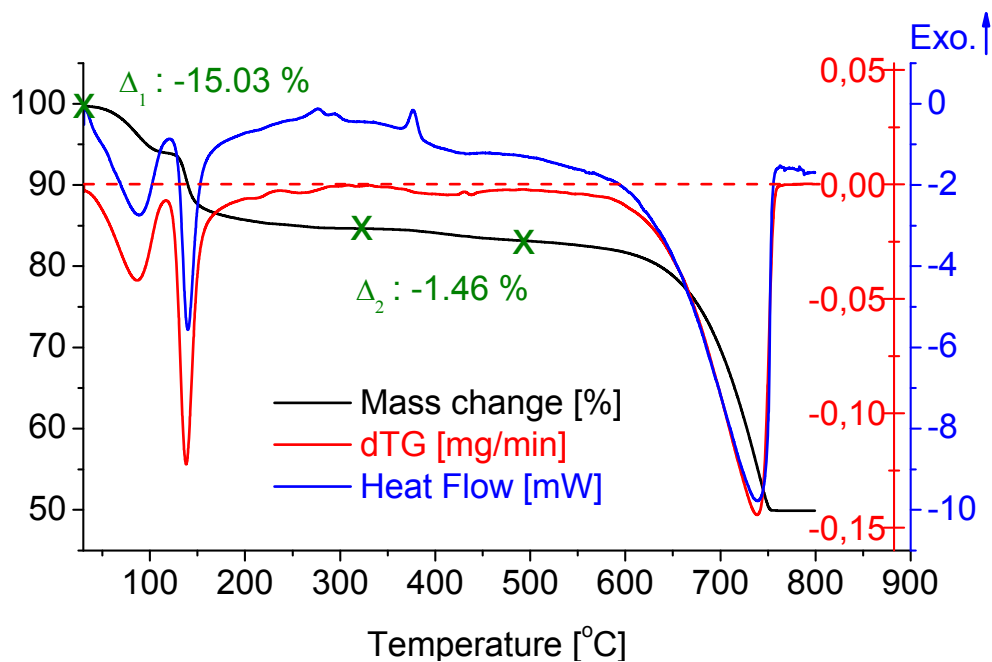
Supplementary Figure S5. Measurement of focal length. The intensity profile 'A' of fluorescence from the selected area in the image 'a' was plot versus the depth. The intensity profiles 'B' of laser were taken from the selected 11 spots in the image of 'b'. The focal length was measured to be $7.2 \pm 0.3 \mu\text{m}$ by adding the distance from the bottom of the microlens to the averaged focal point, $4.4 \pm 0.3 \mu\text{m}$, to the top of the microlens, $2.8 \mu\text{m}$.



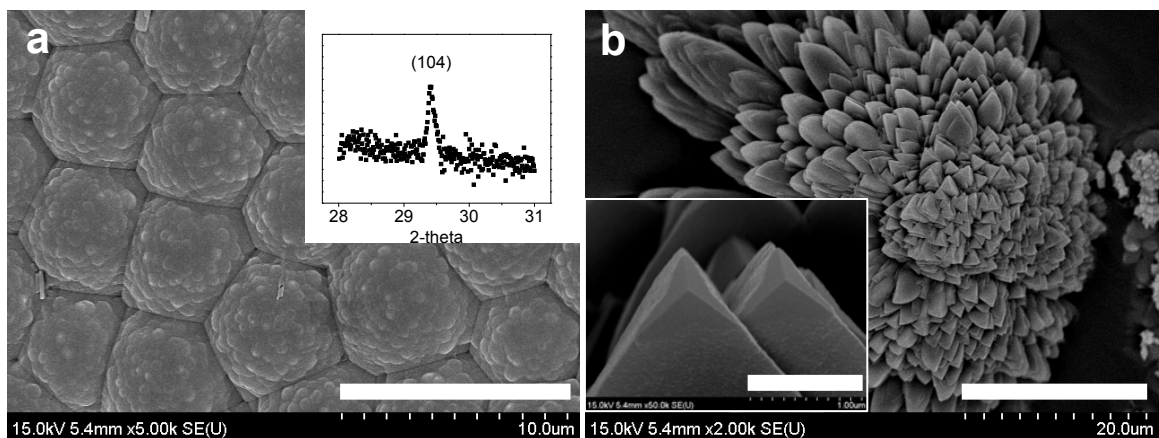
ULE : Upper Lower Edge
LRE : Left Right Edge



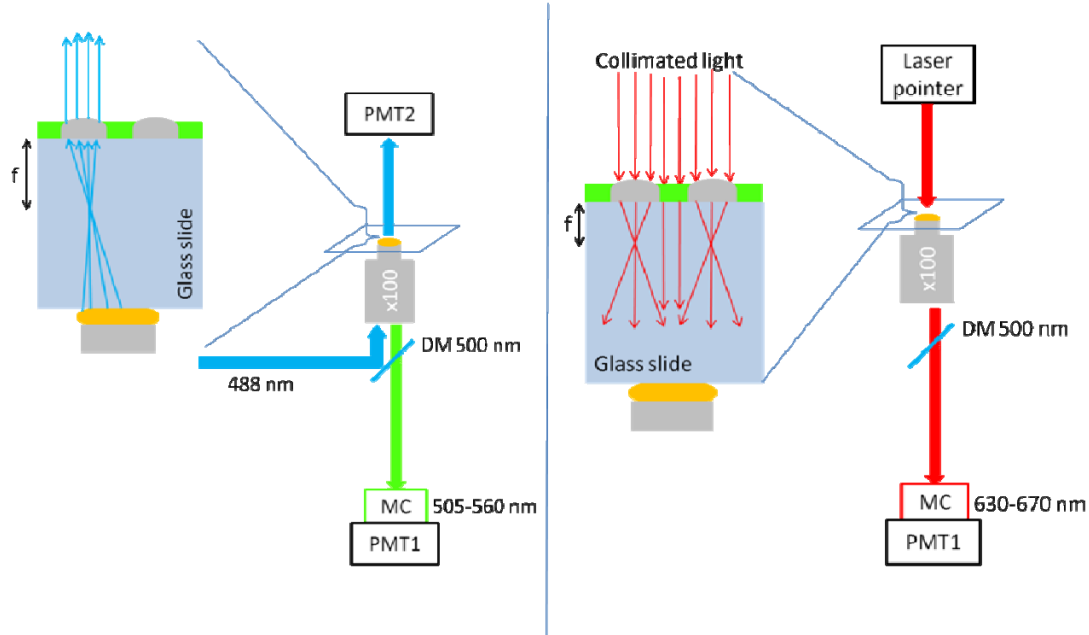
Supplementary Figure S6. Polarized Raman spectra in selected spectral region of carbonate. Blue (0° , ULE) and red (90° , ULE) colored Raman spectra were acquired from the same area of upper lower edge in microlens array but with different incident laser polarization at 0 and 90° deg, respectively. These two spectra show a big difference in intensity. Similarly, fuchsia (0° , In) and black (90° , In) colored Raman spectra were acquired from the same area of inner part in microlens array but with different incident laser polarization. The direction of the incident laser polarization, however, was found to have no influence on the inner part of the lens. The intensity of carbonate band of calcite in the spectral region $1040 \sim 1125 \text{ cm}^{-1}$ was normalized to that of red (90° , ULE) spectrum to compare the FWHM and peak shift. All the scale bars are $3 \mu\text{m}$.



Supplementary Figure S7. Thermogravimetric analysis with differential scanning calorimetry (TGA-DSC) of CaCO₃ microlens structures. TGA shows the weight loss (water) by 15.03 % , which corresponds to about 1 mole of water per 1 mole of calcium carbonate. The weight loss by 1.46 % between 300 °C and 500 °C with exothermic heat flow at 360 °C is due to decomposition of organic component in microlens array.



Supplementary Figure S8. Crystal growth of CaCO₃ structures through further reaction in the solution. a,b, SEM images of CaCO₃ structures after 4 hrs and 24 hrs of reaction, respectively. Submicron-sized structures (a) and (104) facets developed on the crystals (b) which were grown on the hemispherical CaCO₃ structures. WAXS analysis in the inset of (a) shows weak intensity of (104) the peak. The scale bars in (a), (b) and inset of (b) are 10, 20 and 1 μm, respectively.



Supplementary Figure S9. Schematic illustration of the experimental setup for the characterization of the focal length. The sample is mounted on the microscope stage of a commercial epi-fluorescence Laser Scanning Confocal Microscope (Leica). On the left part, the light from a laser emitting at 488 nm is used to excite the sample through a microscope objective (oil immersion 100 ×, 1.4 NA, Leica). The fluorescent light emitted by the fluorescent chitosan (green structure between the microlenses drawn in grey on the magnified schematic of the sample) is spectrally selected between 505 and 560 and recorded by a PMT. This allows the position of the microlenses to be determined. On the right of the illustration, the same experimental is kept. However, this time the sample is illuminated by a collimated beam emitted by a laser pointer secured on top of the microscope stage, perpendicularly to the microscope slide. The light is collected through the same optical path and recorded by the same PMT in the wavelength range 630 to 670 nm. This was used to characterize the optical properties of the microlenses. Particularly, the focal length could be calculated using the combination of images acquired using the setup shown on the left and on the right of the illustration.